Exploring ICA for Differentiating Intracavitary Signals Based on Tissue Composition

Raúl Alós[1], Elisa Ramírez[1], Samuel Ruipérez-Campillo[2], Raúl Llinares[1], Francisco Castells[1], Jakub Hejč[3], Martin Pešl[3], Zdeněk Stárek[3], José Millet[1]

[1] ITACA Institute, Universitat Politècnica de València, Valencia, Spain
[2] Swiss Federal Institute of Technology Zurich (ETHz), Zurich, Switzerland
[3] Brno Hospital, Czech Republic

Abstract

Precise characterization of the cardiac tissue is crucial for diagnosing and treating arrhythmias. In particular, detecting the spatial distribution of fibrotic tissue is key for the understanding of propagation patterns and underlying mechanisms. Although the recent high-density catheters provide enhanced mapping capabilities, difficulties still exist in evaluating tissue properties. In the context of intracardiac signals, the statistical technique of independent component analysis (ICA) has been mainly used for noise and artifact removal. We propose a novel application of this technique for the discrimination of the cardiac tissue, using unipolar electrograms (EGMs) acquired during sinus rhythm, collected from a patient with recurrent atrial fibrillation. Three sets of 16 signals were used, each with an increment in the presence of signals belonging to fibrotic tissue. The analysis carried out using the FastICA algorithm has allowed determining, for the three sets of signals, a set of discriminative ICA loadings and sources between the two types of tissue included. Results obtained from the groundtruth show that the presented novel multivariate approach holds potential as an additional tool for tissue characterization and discrimination under different conditions of atrial tissue.

1. Introduction

The precise characterization of the electrophysiologic substrate is fundamental for understanding and managing cardiac arrhythmias [1], such as atrial fibrillation (AF) and ventricular tachyarrhythmias. These arrhythmogenic substrates often involve fibrotic regions, leading to abnormal conduction patterns that contribute to the initiation and maintenance of arrhythmias. In particular, low-voltage areas (LVAs), which are typically associated with regions of slow conduction, are key markers of arrhythmogenic atrial tissue and are frequently targeted during ablation procedures [2].

To accurately map these regions, high-density catheters equipped with multielectrode arrays have become increasingly important in clinical practice [3]. These catheters provide detailed activation maps, allowing for the assessment of conduction velocity and other electrical properties related to tissue heterogeneity. Despite advancements in electroanatomic mapping technologies, discrepancies remain in the detection of LVAs, difficulting the identification of potential ablation targets [4].

On the other hand, ICA has been used traditionally in this context for filtering unipolar EGMs [5, 6], particularly due to its sensitivity to certain artefacts, such as the ventricular far-field (VFF). However, in other studies, it has been proposed as a statistical tool for electroencephalography (EEG) electrode classification [7] and for group difference enhancement [8].

In this study, we propose the use of ICA as a technique for the classification of intracavitary signals based on tissue type, aiming to improve the identification of arrhythmogenic substrates in cardiac mapping.

2. Materials

The unipolar EGMs that form the basis of the database used were acquired by the Electrophysiology Laboratory of the International Clinical Research Center (ICRC) in Brno, Czech Republic. A high-density catheter (Advisor™ HD Grid Mapping Catheter, Abbott, USA) was used for recording in a patient with recurrent AF. This sensor is characterized by a 4 x 4 structure of unipolar electrodes with an interelectrode distance of 4 mm. A sampling rate of 2034.5Hz was set, and the EGMs were acquired for 1 second.

Based on the identification of healthy and fibrotic tissue by electrophysiologists, three subsets of 16 unipolar signals were selected, each with a gradual increase in the percentage of healthy tissue (37.50%, 50.00%, and 75.00%)

within the catheter position.

3. Methods

The workflow followed in the methodology is shown below (Figure 1).

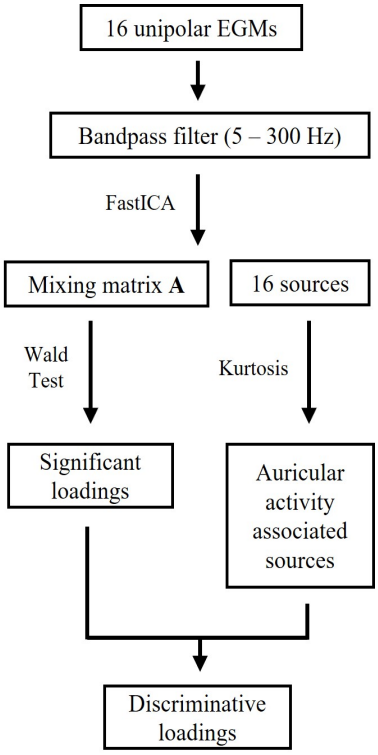

Figure 1. Block diagram illustrating the workflow followed in order to obtain the discriminative loadings.

3.1. Signal preprocessing and ICA

As a preliminary step, each subset of unipolar signals was filtered using a 4th-order band-pass Butterworth filter with cutoff frequencies between 5 and 300 Hz, in order to remove baseline drift and any other artifacts. An example of one of the 16 preprocessed unipolar EGM subsets analyzed is shown in Figure 2.

ICA was then applied to each subset separately. This blind source separation technique allows for the extraction of a set of N independent sources $s(t) \in \mathbb{R}^{\mathbb{N}}$ from M observed signals $x(t) \in \mathbb{R}^{\mathbb{M}}$. The mixing model [9] is expressed as follows:

$$x(t) = A \cdot s(t) \tag{1}$$

Where $A \in \mathbb{R}^{\mathbb{M}\times\mathbb{N}}$ is the mixing matrix to be estimated, with its coefficients representing the weighting of each source in the reconstruction of the original signals. The

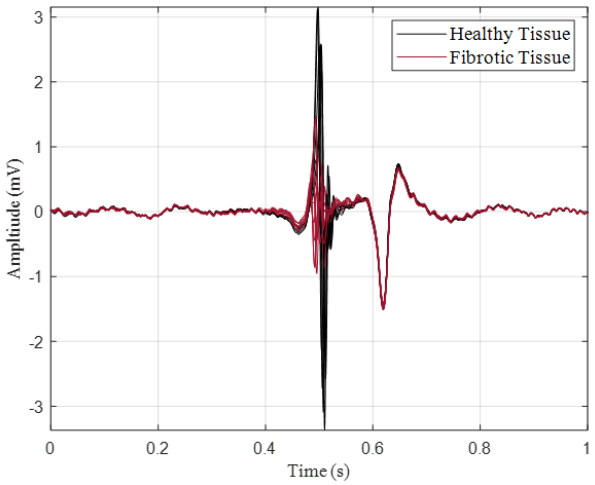

Figure 2. Filtered subset with 37.50% of healthy tissue unipolar EGMs. Healthy signals are coded in black lines and fibrotic signals, in red lines.

algorithm selected in this study was FastICA [10], which focuses on obtaining each source by maximizing its non-Gaussianity, using measures such as negative entropy or kurtosis. In this case, we opted to use the deflation approach and *pow3* as the nonlinearity function, and up to 16 sources were obtained for each analyzed subset.

3.2. Estimation of discriminative loadings

Atrial activity (AA) related components were selected considering the maximization of statistical independence in the FastICA algorithm, as mentioned earlier. Although visual analysis is useful in the detection of AA associated sources, the highest value of kurtosis was used, as depicted in Figure 1.

Given the focus on the mixing matrix's loadings for tissue type differentiation, a Wald test for the mixing coefficients [11] was conducted. Thus, the hypotheses that were tested are the following:

$$H_0 : a_{mn} = 0 \quad versus \quad H_1 : a_{mn} \neq 0 \tag{2}$$

Where a_{mn} represents each coefficient of A and we test if each of them can be considered zero or not. The Wald statistic used was:

$$\frac{\hat{a}_{mn}^2}{avar\left(\hat{a}_{mn}\right)} \tag{3}$$

Where $avar\left(\hat{a}_{mn}\right)$ denotes the asymptotic variance of $\hat{a}_{mn}$, defined in more detail in [11]. Hence, under H_0, the Wald estimate asymptotically approximates to a chi-square distribution with one degree of freedom. The significance level established was 5%. This ensures the identification

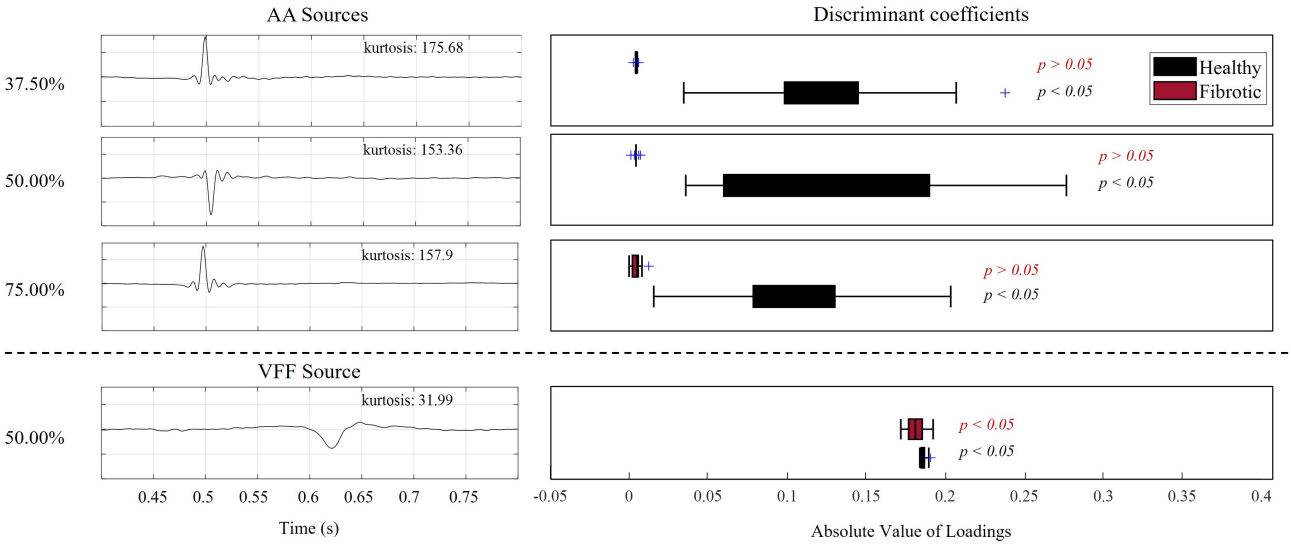

Figure 3. Results of the identification of the AA sources (left) for each subset and the boxplots and statistical analysis of its loadings (right) depending on tissue type (black for healthy, red for fibrotic). One VFF source is placed below for reference.

of independent sources with a statistically significant representation in the unipolar signals. If differences exist between these signals, such as the type of tissue they belong to and its influence on amplitude or morphology, the Wald test would provide a discriminative perspective.

Finally, the ability of the discriminative loadings to classify each sensor was assessed by examining the correlation between these loadings and the ground truth.

4. Results

The results obtained after following the workflow specified earlier are shown in Figure 3. The sources identified with the highest kurtosis (Figure 3, left) coincide temporally with AA, using ventricular far-field (VFF) activity from one of the subsets as a reference. Focusing on the loadings corresponding to these sources (Figure 3, right), both the absolute mean and standard deviation are higher in the coefficients of signals belonging to healthy tissue, in contrast to fibrotic tissue, where the weights have values close to zero. Additionally, statistically significant loadings are observed in the electrodes belonging only to healthy tissue, since the p-values are less than 0.05, which have been referred to as discriminative loadings. In contrast, the loadings of the source associated with VFF are statistically significant regardless of the tissue type.

Figure 4 shows the correlation between the grouped discriminative loadings of the AA sources and peak-to-peak amplitude of the atrial interval of the three subsets. The Pearson correlation coefficient r is 0.81 between the proposed parameter and the ground truth, where the healthy signals are characterized by higher peak-to-peak amplitude values and greater absolute values of loadings.

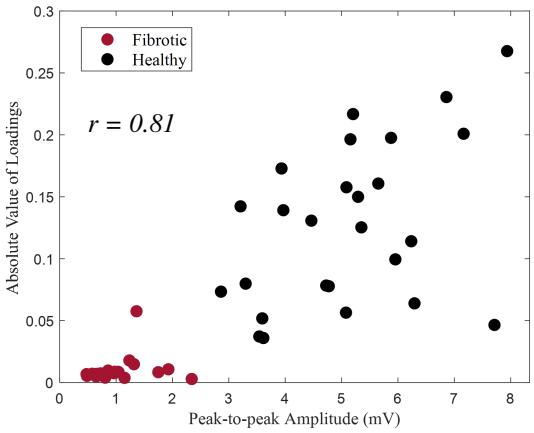

Figure 4. Pearson correlation between ground truth (peak-to-peak amplitude) and the absolute value of the discriminative loadings. Healthy signals are coded in black points and fibrotic signals, in red points.

5. Discussion

Our results showed that fibrotic signals are characterized by non-statistically significant loadings in sources associ-

ated with atrial activity. This finding is further supported by the relatively high correlation between the ground truth and the discriminative loadings obtained. Also, the differences observed between tissue types are consistent, independently of the percentage of healthy tissue in the sample, and the VFF source used as a reference proves that the statistical differences between healthy and fibrotic loadings are not spurious.

For this reason, the results of the proposed analysis demonstrate that ICA contains sufficient information to assist in the classification of healthy and fibrotic signals and further characterization of the discriminative sources. Furthermore, it is believed that this principle can be applied not only to LVAs, as in the present study, but can also be extended to any independent source of interest where representativeness across the sampled tissue is required. (e.g., fractionated complexes, artifacts).

Although the analysis was conducted from a supervised perspective, the threshold used for classification is based solely on statistical significance. This value could be optimized if the model is validated or reduced through certain corrections such as Bonferroni.

Additionaly, the identification of discriminative loadings and sources would be useful for creating signal archetypes for each patient through the respective reconstructions.

Finally, future studies should consider comparing the statistical technique applied with a robust bootstrapping approach [7], as well as validating the analysis provided in this study with a larger and more heterogeneous dataset.

6. Conclusion

This study presents a novel application of ICA for the discrimination of cardiac tissue using unipolar EGMs. The results demonstrate that ICA can effectively differentiate between healthy and fibrotic tissue, as evidenced by the discriminative loadings and their strong correlation with the ground truth. The methodology showed that signals from fibrotic tissue are characterized by non-statistically significant loadings, whereas healthy tissue exhibits higher and more significant loadings in atrial activity sources. This distinction is consistent across varying proportions of healthy and fibrotic tissues, underscoring the robustness of the approach.

Acknowledgments

This work was funded by PID2022-142514OB-I00 (National Research Program, Ministry of Science and Innovation, Government of Spain) and CIBERCV CB16/11/00486 (Carlos III Health Institute).

References

[1] Cesario DA, Vaseghi M, Boyle NG, Fishbein MC, Valderrábano M, Narasimhan C, Wiener I, Shivkumar K. Value of high-density endocardial and epicardial mapping for catheter ablation of hemodynamically unstable ventricular tachycardia. Heart Rhythm 2006;3(1):1–10.

[2] Kottkamp H, Bender R, Berg J. Catheter ablation of atrial fibrillation: how to modify the substrate? Journal of the American College of Cardiology 2015;65(2):196–206.

[3] Deno DC, Balachandran R, Morgan D, Ahmad F, Massé S, Nanthakumar K. Orientation-independent catheter-based characterization of myocardial activation. IEEE Transactions on Biomedical Engineering 2016;64(5):1067–1077.

[4] Kaseno K, Hasegawa K, Miyazaki S, Mukai M, Aoyama D, Nodera M, Hirano K, Otake M, Nomura R, Miyahara K, et al. Discrepancy between carto and rhythmia maps for defining the left atrial low-voltage areas in atrial fibrillation ablation. Heart and Vessels 2021;36:1027–1034.

[5] Abdi B, Hendriks RC, Van Der Veen AJ, De Groot NM. Ventricular activity signal removal in atrial electrograms of atrial fibrillation. In 12th International Conference on Bio-Inspired Systems and Signal Processing, BIOSIGNALS 2019-Part of 12th International Joint Conference on Biomedical Engineering Systems and Technologies, BIOSTEC 2019. SciTePress, 2019; 179–184.

[6] Saha S, Hartmann S, Linz D, Sanders P, Baumert M. A ventricular far-field artefact filtering technique for atrial electrograms. In 2019 Computing in Cardiology (CinC). IEEE, 2019; Page–1.

[7] Basiri S, Ollila E, Koivunen V. Enhanced bootstrap method for statistical inference in the ica model. Signal Processing 2017;138:53–62.

[8] Sui J, Adali T, Pearlson GD, Clark VP, Calhoun VD. A method for accurate group difference detection by constraining the mixing coefficients in an ica framework. Human Brain Mapping 2009;30(9):2953–2970.

[9] Hyvärinen A, Oja E. Independent component analysis: algorithms and applications. Neural Networks 2000;13(4-5):411–430.

[10] Hyvärinen A, Oja E. A fast fixed-point algorithm for independent component analysis. Neural Computation 1997; 9(7):1483–1492.

[11] Shimizu S, Hyvärinen A, Kano Y, Hoyer PO, Kerminen AJ. Testing significance of mixing and demixing coefficients in ica. In International Conference on Independent Component Analysis and Signal Separation. Springer, 2006; 901–908.

Address for correspondence:

Raúl Alós Maldonado
ITACA Institute, Camino de Vera, S/N, 46022, Universitat Politècnica de València, Valencia, Spain
raulalosmald@gmail.com